Development of novel phospholipids-based ultrasound contrast agents intended for drug delivery and cancer theranostics

2016

Rodi Abdalkader

Content

Preface

Theranostics is a term that refers to the combination of therapy and diagnostics so that for example the same particle can both be used for finding a tumour and deliver drugs to treat it. Ultrasound (US) imaging is well-known and safe diagnostic tool that is widely used in many different applications. A limitation of US imaging is the difficulty in differentiating the blood vasculature from the surrounded tissues and therefore US contrast agents (UCAs) are often used for enhancing the contrast signal in the blood vasculature. UCAs are usually made of hydrophobic gases such as perfluorocarbons (PFCs) stabilized in bubble form by biocompatible shells. Recently, not only micro- and nanometer-sized gas bubbles but also liquid nanodroplets that can form gas bubbles *in vivo* (also called phase shift acoustic nanodroplets (PSANDs)) have been proposed. Gas cored UCAs usually have poor *in vivo* stability and by using liquid droplets instead that can be shifted into gas when it is needed, an attractive option can be introduced. After being used for diagnosis for many years, UCAs have recently also been used for enhancing the delivery of drugs and genes through the cavitation effects when combined with therapeutic US (TUS). However, most of the reported UCAs were investigated for imaging or for therapy separately. For theranostic applications, the balance between therapeutic and diagnostic characteristics will be critical. For instance, theranostic UCAs should give image enhancement and then often be simultaneously activated by TUS at the target site. This means they need high contrast signal and sufficient drug payload in one carrier and the stability has to be good enough for reaching the target but not too much good for the TUS activation. To solve this dilemma I have focused on three main aspects of perfluorocarbon carrier systems, first, the employment of phospholipids for stabilizing the UCAs, second the utilization of different hydrophobic

PFCs, and third, the development of suitable preparation method that is well designed for making theranostic UCAs. Phospholipids are biocompatible amphiphilic molecules that are the main component in cell membranes and have been frequently used in the biomedical research. Compared to other shell materials (e.g., polymers that form rigid shells), phospholipids can maintain better stability and resonant properties in UCAs due to their high flexibility and ability to adapt when an US wave leads to bubble oscillation. Moreover, drug and nucleic acids can be loaded into phospholipids shells easily by using the charge properties that lead to complex formation between drug molecules and the phospholipids' hydrophilic head groups. The other component, the PFCs are essential for US contrast signal enhancement. They have different physicochemical properties depending on structure and molecular weight that consequently affect UCAs size distribution, stability, and echogenicity. Moreover, the selection of proper preparation methods is also important. For example, sonication is a well-known method for preparing UCAs. However, it is not preferable in the case of thermo sensitive material and, thus, an alternative method such as mechanical agitation would be used.

In this thesis, I have developed several types of novel phospholipid-based UCAs. I aimed to show the merits and limits of each formulation and how we can improve these limits for better theranostic use. This included *in vitro* and *in vivo* evaluation of theranostic characteristics of these UCAs and based on that, the potential use of these carriers was then investigated for the purpose of gene delivery and cancer theranostics.

Chapter I

Formulation and evaluation of nano- and micro-sized phospholipids-based theranostic ultrasound contrast agents

Section I. 1

The development and characterization of mechanically formed bubbles

Section I. 2

The development of mechanically formed bubbles loaded with doxorubicin

I.2.1. Introduction

Doxorubicin (DOX) is one of the most used anti-cancer agents for a variety of solid tumours such as osteosarcoma, leukaemia, Hodgkin`s lymphoma, and breast cancer [1]. The combination of DOX and bubbles with TUS irradiation has been found to enhance DOX uptake in cells through sonoporation [2, 3]. Also, many reports have shown the possibility of loading DOX into bubbles by electrostatic interactions [4, 5].

However, most of these reports have focused on the therapeutic use of the formulations. The diagnostic potential has been less in focus. For cancer theranostic applications, both DOX and perfluorocarbons (PFCs) gas should be stably encapsulated in the same bubbles. Therefore obtaining such balance is crucial for better theranostic use.

In Section I 1, I showed that homogenous phospholipid-based bubbles could be produced by using a mechanical agitation method. Also, my results indicated that bubbles made especially with perfluopropane gas (PFP) had narrow size distribution and good stability for a long time. Moreover, it was reported that anionic phospholipid distearoylphosphatidyl glycerol (DSPG) incorporated in the bubbles could enhance their half-life both *in vitro* and *in vivo* [6]. At the same time, DSPG can offer a platform for DOX loading in bubbles shells mainly through electrostatic interactions. Taking all of these in consideration, I expected that DOX-loaded bubbles (DLBs) can be formed by using the previous method.

In this section, I optimised the conditions required for the preparation of stable

DLBs by using mechanical agitation. The balance between the encapsulation of DOX and PFP gas was studied. Also, the *in vitro* theranostic characteristics such as echogenicity and DLB's destructibility by TUS were tested as well.

I.2.2. Materials and methods

I.2.2.1. Phospholipids

DSPG, 1, 2-dipalmitoyl-sn-glycero-3- phosphatidylcholine (DPPC) and PEG_{2000}-DSPE were purchased from Avanti Polar Lipid Inc. (Alabaster, AL, USA) and NOF Co. (Tokyo, Japan).

I.2.2.2. DOX-liposome and DLBs preparation

DPPC, DSPG and PEG_{2000}-DSPE in a 70:25:5 molar ratio were dissolved in a MeOH: chloroform mixture, followed by evaporation of the solvents in a rotary evaporator at 25°C for 30 min. This was further dried under vacuum at room temperature overnight. Ten mg of lipid film was hydrated with 3 ml of 5% glucose solution (containing 2 mg of DOX) at 65 °C for 60 min under mild agitation, to obtain a lipid dispersion (liposomes). The final lipid concentration after hydration was adjusted to 3 mg/ml. For preparing bubbles, 0.5 ml of the lipid dispersion was added to a 5 ml sterilised vial. The air in the vial was replaced with PFP gas (Takachiho Chemical Industries Co., Tokyo, Japan) and after capping 6 ml of PFP was injected. A shaking machine (Ultra Mate 2, Victoria, Australia) was used to obatin bubbles. The temperature in the samples was measured after agitation using a needle-type thermometer (Custom Co., Tokyo, Japan). PFP content measurment was performed as reported in Section I 1. The particle size and zeta potential of the liposomes and bubbles were determined using a Zetasizer Nano ZS instrument (Malvern Instruments Ltd., Worcestershire, UK).

I.2.2.3. DOX binding efficiency

To determine the binding efficiency of DOX in DLBs, a sample consisting of 0.5 ml DLB's dispersion (1.65 mg lipid and 0.33 mg DOX) was centrifuged at 16,000 g for 2 min. Then the sample was divided into three fractions: a foaming cake at the top which contained DLBs; a pellet at the bottom, which contained liposomes; and in-between a solution containing free DOX. The fractions were collected, and then the concentration in each fraction was determined by measuring fluorescence of DOX with an excitation wavelength of 480 nm and emission wavelength of 590 nm (FluoroMax4, Horiba, Ltd., Kyoto, Japan).

I.2.2.4. *In vitro* echogenicity

The DLBs were injected into a beaker filled with 500 ml of degassed distilled water at 37°C under magnetic stirring. Ultrasound contrast enhancement was observed using an ultrasonography system (Vevo 2100, Visual Sonics, Inc. Toronto, Canada). For examination of DLB's destruction by higher energy TUS irradiation, an external TUS probe at an intensity of 2 W/cm² was used. The process of TUS burst was repeated until most of the DLBs had disappeared.

I.2.3. Results

I.2.3.1. Size and morphology of DLBs

The size of the DLBs was adjusted by changing the agitation time of the shaking machine. Agitation for 60 s was sufficient to produce bubbles with an average diameter of 1 μm (Table 1). During this procedure, the temperature did not exceed 26.7°C.

Table 1. Mean particle size and zeta potential of liposomes and bubbles. n = 3; mean ± SD

	Mean particle size (nm)	Zeta potential (mV)
Unloaded liposome	250 ± 1	-0.076 ± 0.02
DOX-loaded liposome	270 ± 6	0.038 ± 0.02
Unloaded bubbles (ULBs)	1051 ± 4	-0.066 ± 0.04
DOX-loaded bubbles (DLBs)	1022 ± 5	0.31 ± 0.01

I.2.3.2. Gas leakage

PFP gas retention was enhanced by the increasing of DOX content from 10 to 82%. The time course of gas leakage showed that at a DOX concentration of 10%, PFP gas leaked faster than bubbles without DOX. However, at levels of 42% and 82% (equivalent to 1:1 mole of DOX: DSPG) DOX enhanced PFP gas retention was evident for at least 30 min at room temperature relative to both ULBs (0 DOX) and the control (saline with PFP) (Fig. 5).

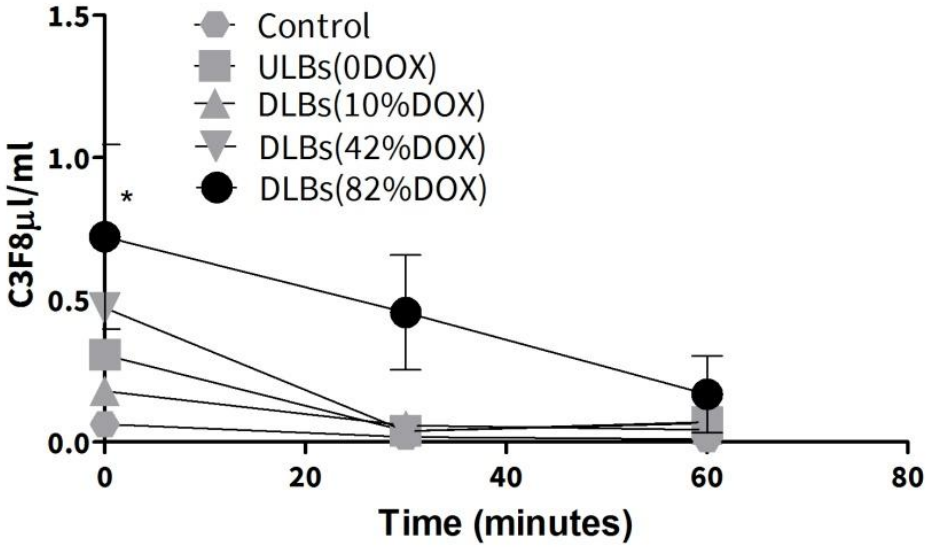

Fig. 5. Time course study of gas leakage from DLBs with different DOX concentrations presented as percentages equivalent to anionic phospholipids. Mean ± SEM. * $P < 0.05$ versus the corresponding control group (saline with PFP gas).

I.2.3.3. DOX loading efficiency

The loaded amount of DOX in DLBs was adjusted to 497.9 ± 17.4 µg/ml (n = 3), and 92.5% of the total DOX was loaded into the DLBs after total separation from free DOX and pellets (Fig. 6A). The fluorescence microscope images indicated successful DOX loading. Images showed spherical bubble in which the DOX signal was observed in the shells (Fig. 6B).

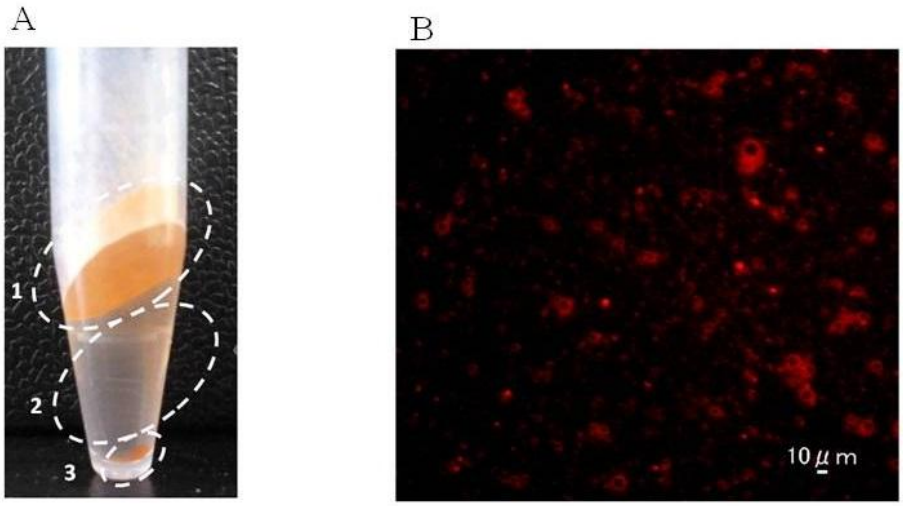

Fig. 6. (A). DLB's separation through buoyancy effects after centrifugation: (1) DLBs, (2) free DOX, and (3) pellets of phospholipids aggregate with doxorubicin. (B). Fluorescence images based doxorubicin detection (scale bar of 10 µm).

I.2.3.4. *In vitro* DLB's echogenicity and destructibility

The echogenicity of DLBs was assessed *in vitro* after injection of the freshly prepared DLBs at 37°C. The brightness mode of ultrasonography showed a high signal from the DLBs even after 10 min (Fig. 7A). The acoustic destructibility study for the DLBs demonstrated that TUS irradiation from 40 to 60 s caused a significant decrease in the ultrasonography video intensity as most of the bubbles had been destroyed (Fig. 7B).

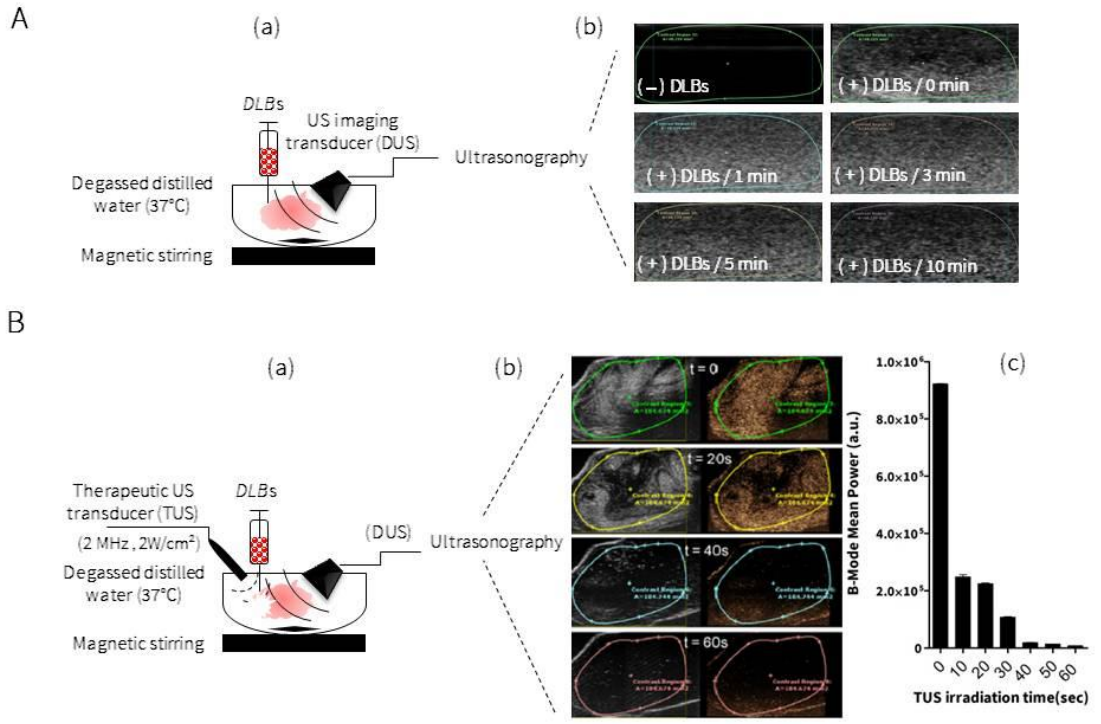

Fig. 7. (A). DLB's echogenicity *in vitro*: (a). US imaging experimental setup. (b). Images of DLBs in brightness mode. (B). *In vitro* DLB's acoustic destructibility. After the injection of DLBs, US echo imaging was performed and then the TUS destruction beam was applied from the external probe at an intensity of 2 W/cm^2: (a). US imaging experimental set up. (b). Images of DLB's brightness and contrast mode after the application of TUS irradiation. (c). Graph presenting DLBs contrast signal regression after 6 volumes of TUS irradiation (10 s each).

I.2.4. Discussion

Many studies have reported on the different methods by which DOX was successfully prepared and tested for tumour therapy in combination with TUS irradiation [3, 7]. Although most of the previous approaches achieved high therapeutic efficacy *in vitro* and *in vivo* [4, 5, 8], there is a little evidence regarding their potential role in US imaging and whether or not the co-encapsulation of PFP and DOX is effective enough for US contrast enhancement in addition to enhancement of the

therapeutic effect of DOX.

In this study, I examined the potential of the theranostics characteristics of DLBs. The size of DLBs was controlled by agitation and initially, 60 s of agitation was enough for producing bubbles with a good size distribution. This result indicates that the majority of DOX-phospholipids had formed DLBs with high DOX loading efficiency (92.5%).

During this procedure, the temperature did not exceed 26.7°C, suggesting that it is a mild process. This would be beneficial if thermo sensitive compounds are intended to be included in the formulations. The fluorescence images of DLBs revealed spherical shapes in which DOX was bound to the DSPG in the shell through electrostatic interactions between the positively charged DOX and the negatively charged bubbles (Fig. 6).

Since DOX loading and PFP gas retention are critical factors for the successful theranostic application, I attempted to investigate a possible relationship between PFP gas retention and the amount of DOX intercalated with DSPG in the bubbles. Gas chromatography was used to quantify the amount of PFP gas in the DLBs at different DOX to DSPG ratios. As shown in Fig. 5, a higher DOX loading enhanced PFP gas retention in the DLBs. These observations suggested that not only DSPG incorporation in bubbles but also the interaction between DSPG and doxorubicin is an important factor for stable PFP encapsulation.

TUS burst for a period of 60 s at an intensity of only 2 W/cm^2 was sufficient to induce a significant decrease in the contrast signal of DLBs; the presumption was that destruction of the DLBs most likely occurred as a result of bubble cavitation (Fig. 7B). It can be concluded that TUS burst caused the bubble destruction through the

comparison between Fig. 7A and Fig. 7B. As shown in Fig. 7A, the same DLBs monitored with lower energy DUS without burst and bubbles remain after 10 min whereas the 2 W/cm^2 burst destroyed virtually all bubbles in 40 s.

In conclusion, DLBs clearly showed therapeutic and diagnostic chracteristics due to high DOX loading into bubbles which also enhanced PFP gas retention. Additionally, DLBs could effectively interact with both TUS and DUS. Therefore, DLBs has the fundamental characteristics to be further utilised in cancer theranostics.

Section I. 3

The development of freeze-dried doxorubicin loaded bubbles

Section I. 4

Phospholipid-based phase shift acoustic nano-droplets

Chapter II

Application of phospholipids-based ultrasound contrast agents in gene delivery and cancer theranostics

Section II. 1

The effective use of mechanically formed bubbles in enhancing the gene delivery

Section II. 2

Evaluation of the theranostic potential of doxorubicin loaded bubbles in tumour bearing mice

II.2.1. Introduction

Cancer theranostics is a portmanteau of cancer therapy and cancer diagnostics. It is usually done through the co-delivery of the anti-cancer agents together with the contrast imaging agents. The aim of such strategy is the active monitoring of cancer progress during therapy [9, 10]. A more advanced approach is to put the therapeutic function and the diagnostic function in the same carrier. In such a case trade-offs between the diagnostics and therapeutic functions may have to be done to get balanced theranostic characteristics. The combination between UCAs and TUS/DUS can provide a novel, non-invasive platform for cancer theranostics [11, 12]. The main benefits of using TUS activated bubbles for various therapeutic applications are that the effect can be localised to primarily the tissues that are exposed to TUS and that the bubbles are also possible to be detected with DUS imaging. The imaging aspect can be used for *e.g.* examination of tumour neovasculature but also the treatment itself can directly be assessed by *e.g.* monitoring bubble location and bubble destruction in real time at the target site [13, 14]. This concept has already been shown to have potential in many reports in mice with tumour models and results have confirmed that the concentration of anticancer drugs in the tumour can be increased when using such strategy [2].

In section I 2, the preparation of bubble type UCAs that were successfully loaded with high amount of DOX and PFP gas was described. The balance between the contrast gas and DOX loading was successfully achieved. Also, DLBs had high *in vitro* echogenicity in addition to the ability in inducing cavitation effects when combined

with TUS. Therefore, it is expected that DLBs could be an effective theranostic agent in cancer therapy.

In this study, both therapeutic and diagnostic tests were conducted *in vitro* with tumour cells and *in vivo* in tumour bearing mice. That included: DOX accumulation in tumour, tumour volume reduction, animal body weight change, and ultrasonography imaging of DLBs in tumours.

II.2.2. Materials and methods

II.2.2.1. DLBs preparation

Bubbles were prepared as described in Section I 2.

II.2.2.2. Cells

The B16BL6 murine melanoma cell line was obtained from the American Type Culture Collection (ATCC, Manassas, VA, USA). Cells were cultured in Dulbecco's modified eagle medium Nissui Pharmaceutical Co., Ltd., (Tokyo, Japan) supplemented with 10% fetal bovine serum and 100 U/ml penicillin/streptomycin at 37ºC in 5% CO_2.

II.2.2.3. Animals and tumour models

Female 6-week-old C57BL6 mice were purchased from the Shizuoka Agricultural Cooperation Association for Laboratory Animals (Shizuoka, Japan) and female 6-week-old HRI nude mice were obtained from Sankyo Laboratory Service Corporation, Inc. (Tokyo, Japan). For preparing tumour bearing mice, 1×10^6 cells in phosphate buffered saline (PBS) were injected subcutaneously into the left flanks of mice with a 26-gauge needle. Experiments were initiated when tumours reached 5–10 mm in diameter after 9–14 days. All experiments were approved by the animal Experimentation

Committee of the Graduate School of Pharmaceutical Sciences, Kyoto University and by Teikyo University School of Medicine Animal Ethics Committee number 14-027.

II.2.2.4. *In vitro* cellular uptake and anti-proliferative assay

Cellular uptake *in vitro* was evaluated using a confocal microscopy (Nikon, Tokyo, Japan). B16BL6 cells were grown on cover glass slides in 24-well plates (3×10^5 cells/well). DLBs were added to the medium, containing DOX at concentration of 5 µg/ml. Then a 6-mm TUS probe was immersed into the well and TUS irradiation was performed for 60 s (2 MHz; 2W/cm²; 50% Duty; 10 Hz). TUS acoustic parameters were selected based on the previous DLBs destructibility experiment described in Section I 2. Fifteen minutes after the treatment with DLBs and TUS, cells were washed with PBS three times and fixed with 4% paraformaldehyde in PBS; DOX localization in cells was then obtained. The 480 nm filter of the microscope was used to excite DOX and then DOX was detected by the 590 nm detector. The images were processed using ImageJ software.

As for anti-proliferative assay, B16BL6 cells were seeded in 6-well plates (3×10^5 cells/well) for 24 hr; DLBs/ULBs (0 DOX) were added at different concentrations. TUS was applied for 60 s (2 MHz; 2W/cm²; 50% duty; 10 Hz). After treatment, cells were incubated for 5 hr and then the medium was changed and the cells were incubated again for 24 hr. After that the 3-(4,5 sec-dimethylthiazol-2-yl)-2,5-diphenyl tetrazolium bromide (MTT) assay was carried out according to the method as previously reported [15].

II.2.2.5. *In vivo* DOX content in tumours

DLBs (70 µg DOX and 330 µg lipid) in 5% glucose (final volume of 200 µl) were intravenously injected and then immediately tumours were irradiated with TUS for 60 s.

Mice were sacrificed 15 min after the injection of DLBs and subsequently tumours, hearts and livers were harvested, weighed and preserved at −80°C. DOX was extracted by homogenising the tumours with a mixture of isopropanol and 1 M HCl aqueous solution (1:1 v/v) and incubated for 1 hr at 4°C. It was then centrifuged at 13,000 g for 15 min, and the supernatants were recovered for fluorescence detection (FluoroMax4, Horiba, Ltd., Kyoto, Japan). DOX standard series were prepared in non-treated tumour tissues extracts.

II.2.2.6. *In vivo* tumour inhibition and imaging

The first treatment was initiated on the 9^{th} day after tumour cell inoculation and repeated on the 11^{th} and 13^{th} days. Immediately after intravenous administration of DLBs, the tumour site was irradiated for 60 s with TUS (2 MHz; 2W/cm²; 50% Duty; 10 Hz). Tumour volume was measured every 2–3 days using the formula: (major axis×minor axis^2) ×0.5.

HRI nude mice (n = 3) inoculated with B16BL6 melanoma were anaesthetized and placed on an imaging pad; temperature, heart rate and breathing were continuously monitored. DUS imaging was performed as previously described [16]. Briefly, a dedicated small animal high-spatial-resolution imagining liner transducer (16 MHz; gain, 25 dB; dynamic range, 50 dB) (Vevo 2100) was used. Subsequently, DLBs were injected at a dose of 100 µl/mouse (300 µg/ml lipid) and images (460 frames) were obtained before and after injection. The data were analysed by comparing the differences in contrast enhancement signal at tumour sites. For investigating the DLBs path through the tumour vasculature, the maximum intensity persistence analysis (MIP) mode (Vevo 2100) was used.

II.2.2.7. Statistical analysis

All data were analysed as the mean ± SEM. Unpaired, the two-tailed distribution Student's t-test was applied and values of $P < 0.05$ were considered as being statistically significant.

II.2.3. Results

II.2.3.1. *In vitro* DOX uptake and MTT assay

In vitro, DOX delivery was investigated in B16BL6 cells using confocal scanning microscopy. The combination of DLBs with TUS irradiation (Fig. 17A) showed higher cellular accumulation of DOX 15 min after treatment compared with DLBs in the absence of TUS irradiation (Fig. 17B). The combination of free DOX with TUS irradiation did not give high levels of DOX (Fig. 17C).

Unloaded bubbles that has no DOX (ULBs) in combination with TUS irradiation resulted in a decrease in tumour cell viability by about 32.5%, suggesting that there were cavitation effects associated with ULBs in combination with TUS irradiation. DLBs used in the absence of TUS irradiation resulted in a decrease in cell viability of approximately 27%. In contrast, cell viabilities were significantly lower after treatment with DLBs combined with TUS irradiation than those treated with DLBs in the absence of TUS irradiation (1.5 and 3.0 μg/ml DOX) (Fig. 18).

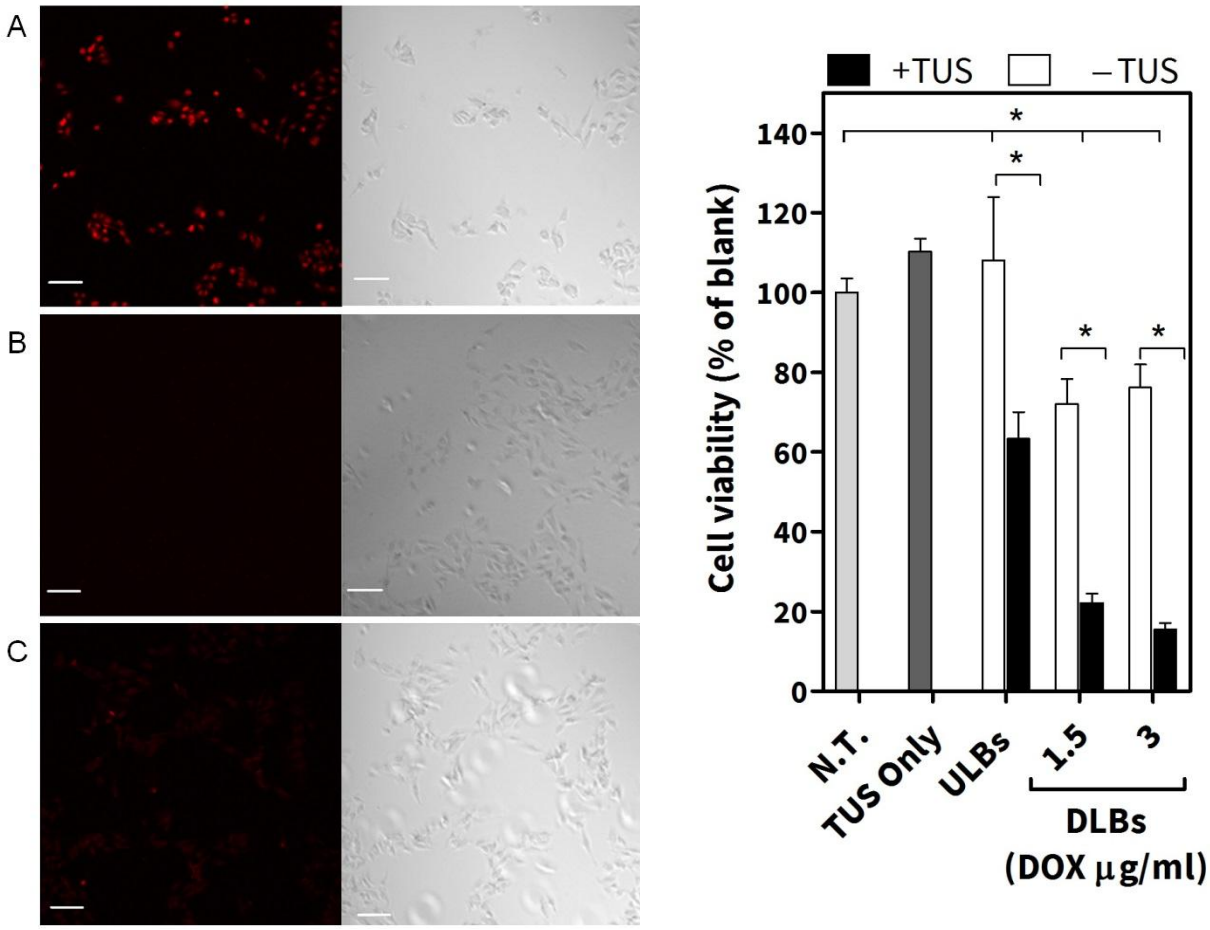

Fig. 17. Confocal laser microscopy images of B16BL6 cells having DOX with various methods. (A) DLBs in combination with TUS irradiation, (B) DLBs in the absence of TUS irradiation and (C) Free DOX in combination with TUS irradiation (scale bar, 50 μm). Cells were treated with DLBs and free DOX in combination with TUS irradiation and then incubated for 15 min prior to the analysis.

Fig. 18. The viability of B16BL6 melanoma cells after treatment with DLBs, ULBs; unloaded microbubbles (0 DOX) and TUS irradiation alone. Each bar represents the mean ± SEM of six experiments. * $P < 0.05$ versus the corresponding groups with no treatment (N.T.).

II.2.3.2. Intratumoral content of DOX in tumour bearing mice

As shown in Fig. 19, the combination of DLBs with TUS irradiation significantly enhanced the intra-tumoral DOX level (0.536 μg/g tissue) as compared with DLBs without TUS irradiation (0.100 μg/g) (Fig. 19A). Conversely, the levels of DOX in liver (Fig. 19B) and heart (Fig. 19C) did not significantly differ between the two groups.

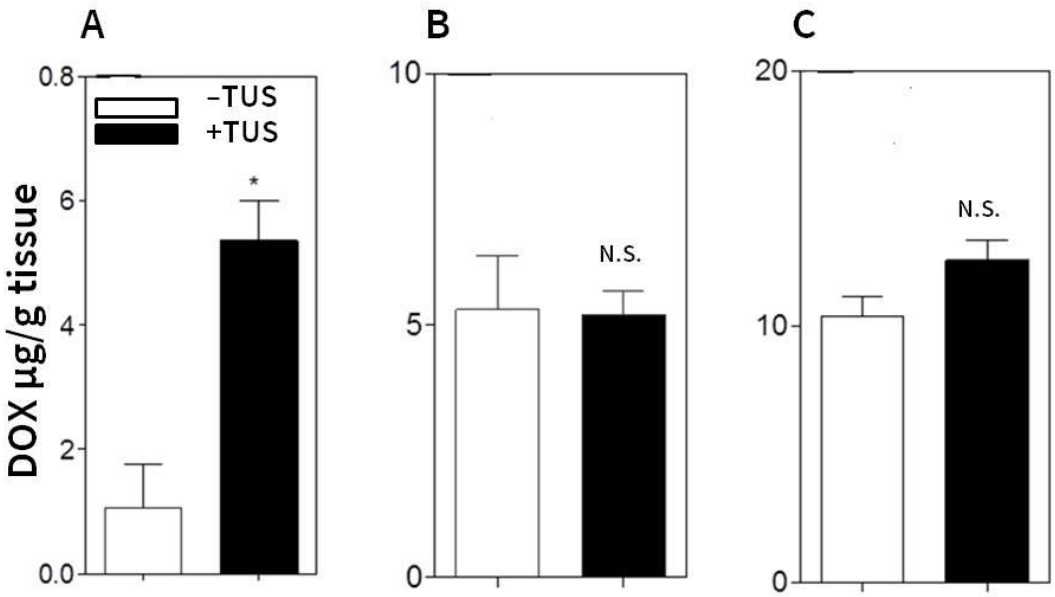

Fig. 19. DOX distribution characteristics after intravenous administration of DLBs with or without TUS irradiation in tumour bearing mice. The DOX content was measured in (A) Tumour, (B) Heart and (C) Liver. Each bar represents the mean ± SEM of five experiments. * $P < 0.05$ versus the corresponding group that received DLBs in combination with TUS irradiation.

II.2.3.3. Tumour growth inhibition and body weight change in tumour bearing mice

By day 27 after tumour inoculation, tumour volume in the control group had aggressively increased (7156 ± 1384 mm^3). The tumour volume was slightly reduced relative to the control group (4663 ± 454 mm^3) in the group of mice treated with DLBs in the absence of TUS irradiation. In contrast, the group of mice treated with DLBs in combination with TUS irradiation, showed significant reduction of tumour growth (2454 ± 175 mm^3) (Fig. 20A). Moreover, treatment with DLBs in combination with TUS irradiation did not cause any significant loss of body weight relative to the control

group (Fig. 20B).

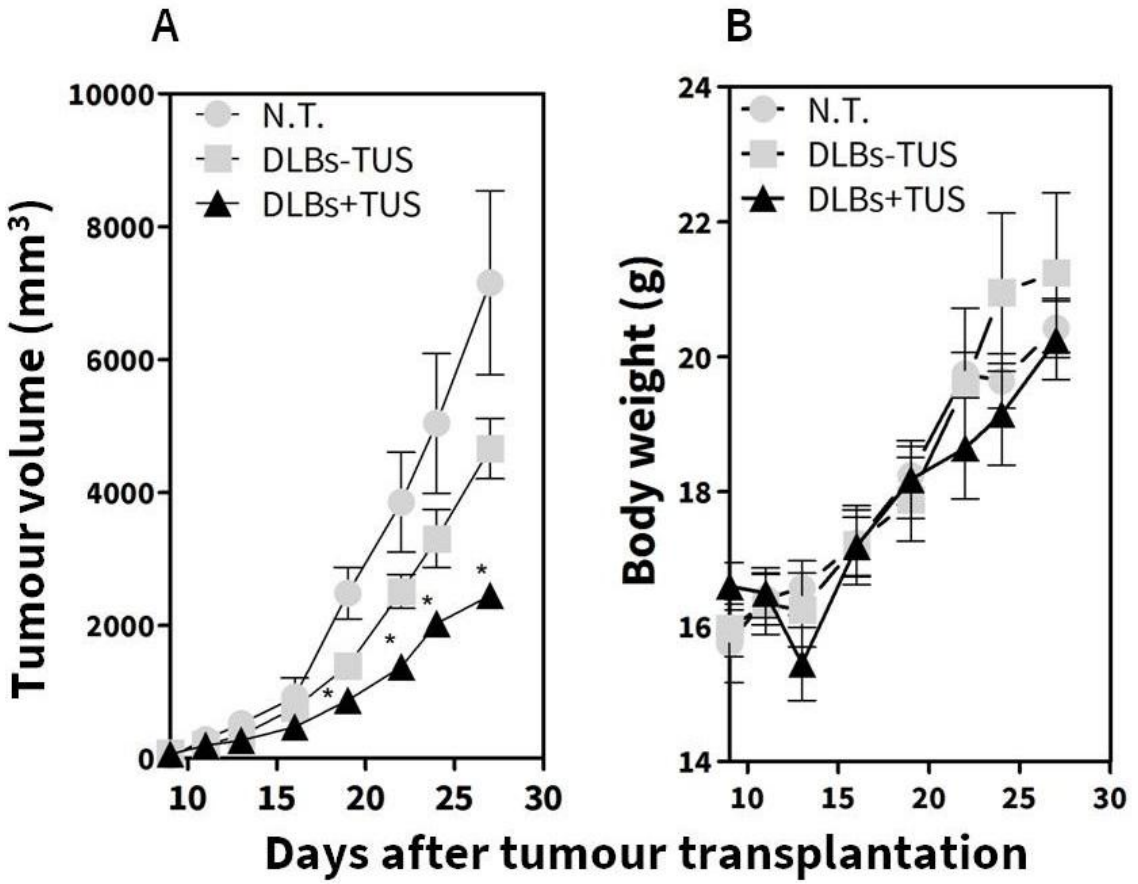

Fig. 20. Effect of DLBs administration with various methods on tumour growth and body weight change. (A). Tumour volume in mice. (B). Mouse body weight. Mice were divided into three groups: control; DLBs only; and DLBs in combination with TUS irradiation. Treatment was performed on the 9th day after tumour transplantation and was repeated on the on the 11th and 13th days. Each bar represents the mean ± SEM of 5–6 experiments. * $P < 0.05$

II.2.3.4. *In vivo* ultrasonography

After 1 min, the intensity of the contrast enhancement signal was gradually reduced (Fig. 21A). The images were analysed by plotting the mean contrast intensity in the tumour area against time after DLB injection (Fig. 21B). The half-life time of intensity decrease of DLBs was estimated to be between 2–3 min. Moreover, the maximum intensity persistence (MIP) analysis clearly revealed the distribution of DLBs in the

tumour vasculature with a clearly distinguishable contrast signal (Fig. 21C).

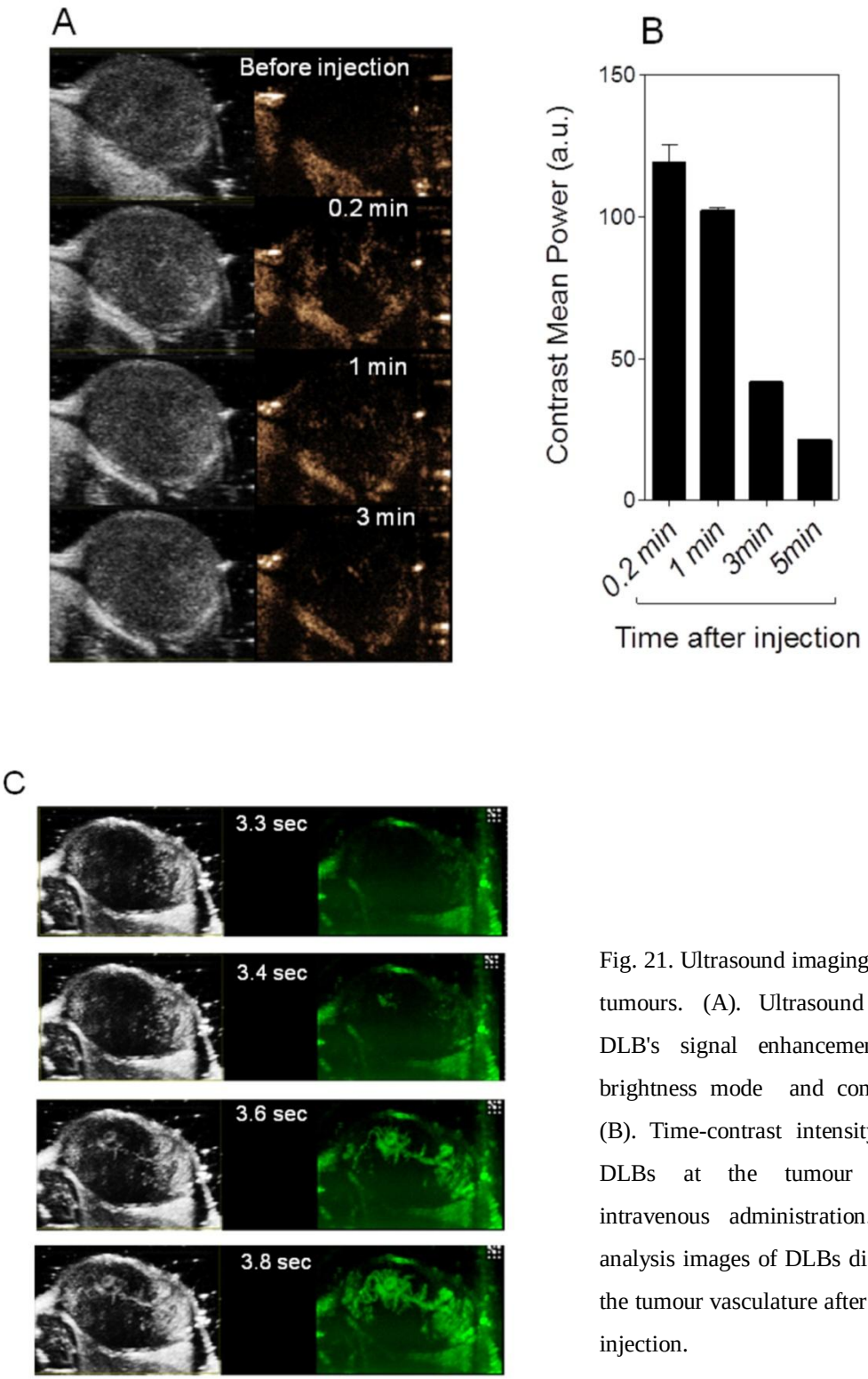

Fig. 21. Ultrasound imaging of DLBs in tumours. (A). Ultrasound images of DLB's signal enhancement in both brightness mode and contrast mode. (B). Time-contrast intensity graph for DLBs at the tumour site after intravenous administration. (C). MIP analysis images of DLBs distribution in the tumour vasculature after intravenous injection.

II.2.4. Discussion

In this section, I demonstrated that DOX uptake in cancer cells was enhanced when DLBs were combined with TUS irradiation, leading to high *in vitro* cytotoxicity and effective *in vivo* DOX delivery (Fig.17). Bubbles in combination with TUS can cause perturbation of the cell membranes and hence enhance drug permeability in a reversible process that lasts for a couple of minutes [11]. Unlike Tinkov and co-workers, I found a significant difference in doxorubicin uptake between DLBs with ultrasound compared with free doxorubicin 15 minutes after treatments [8]. This difference could be due to the experimental conditions like the DOX incubation time. It is well known that DOX is easily taken up by the cells through passive diffusion and the active transport mechanism which means that the long incubation time used by Tinkov *et al* might have lead to a substantial contribution from this way of uptake to the total drug amount [17]. Lentacker *et al* found that after 15 minutes of treating cells with free DOX, the amount of internalised DOX by the cells was much lower than those treated with bubbles loaded with DOX-liposomes [3]. Based on this, minimising the incubation time can be critical for understanding the sonoporation process when bubble cavitation occurs.

In the *in vivo* experiment, it is expected that TUS irradiation at the tumour site leads to DLB's cavitation and DOX release; consequently, the concentration of free DOX was increased in tumour but not in the heart and liver. Furthermore, DLBs in combination with TUS significantly inhibited tumour growth without any reduction in animal body weight. These results suggest that DLBs combined with TUS irradiation at the tumour site could improve treatment accuracy and safety with less systemic side effects including cardiotoxicity.

In the tumour, DOX might have been delivered primarily to the endothelial cells of

the tumour microvasculature. Subsequently, nutrition supply to the tumour would be disrupted due to necrosis caused by dead endothelial cells [18]. However, direct delivery of DOX into tumour cells might have occurred as well. It has been reported that cavitation effects can enhance drug penetration into the tumour by further "opening up" of the endothelial barrier [19].

As shown in Fig. 21, the imaging potential of DLBs was confirmed by DUS ultrasonography imaging, which revealed a high contrast enhancement signal in the tumour area in mice after DLBs administration. Moreover, I showed that the contrast mode signal from DLBs in the tumour vasculature could be clearly distinguished from the surrounding healthy tissues. Pysz *et al* have reported that *in vivo,* the ultrasound imaging signal in tumour bearing mice using MIP algorithm could be used to assess tumour vascularity [13]. That is because a correlation between the *in vivo* MIP values with microvessel density analysis was observed. Therefore, tumour angiogenesis could be monitored by evaluating the MIP analysis of DLBs distribution in the tumour vasculature.

In conclusion, DLBs will function as a theranostic carrier in both *in vitro* and *in vivo*. DLBs stability *in vivo* was enough for conducting the DUS imaging as well as for the delivery of DOX when triggered with TUS. Therefore, these results strongly support the potential use of DLBs as a vasculature probe in tumor theranostics.

Section II. 3

Investigation on the use of liquid cored ultrasound contrast agents for cancer theranostics: Systemic administration route

Section II. 4

Investigation on the use of liquid cored ultrasound contrast agents for cancer theranostics: Intratumoral route

Summary

In this thesis, I have demonstrated that the theranostic characteristics of UCAs can be optimised by including three critical factors. First, the utilisation of phospholipids as shell materials for UCAs. Second, the employment of PFCs as core material in UCAs. Third, the selection of suitable methods for producing theranostic UCAs. Further findings and applications are summarised as follows:

I. Formulation and evaluation of nano- and micro-sized phospholipids-based theranostic ultrasound contrast agents

A type of UCAs was developed by using mechanical agitation of lipids dispersion in the presence of perfluoropropane gas (PFP). The focus was on improving the size distribution and stability. Mechanically formed bubbles (MFBs) were composed of the zwitterionic phospholipid distearoylphosphatidyl choline (DSPC) with a portion of polyethylene glycol (PEG) engraftments. MFBs with PFP had a smaller size (~ 400 nm) compared to those made with perfluorobutane or nitrogen gases. Also, MFBs with PFP were found to be stable with uniform size for 24 hr at room temperature (RT) and at 4 °C bubbles could be preserved for 90 hr. By using a similar method, doxorubicin loaded bubbles (DLBs) were also prepared. The DLBs were prepared by mechanical agitation of phospholipid dispersion in the presence of PFP gas. The anionic phospholipid distearoylphosphatidyl glycerol (DSPG) was selected to bind doxorubicin to the bubbles by electrostatic interaction. Drug loading was ≥92% and bubbles had an average size of about 1 μm. The PFP was retained in the bubbles at least 30 min at RT. *In vitro* ultrasonography also showed that DLBs have high signal even after 10 min and when TUS irradiation was applied most of the bubbles were destroyed. This indicated that

DLBs were presumably destroyed due to cavitations effects. Phase shift acoustic nanodroplets (PSANDs) were also prepared by using a similar phospholipid composition as in the MFBs. The PSANDs were prepared in a two step process that consisted of mixing liposomes with liquid perfluoropentane (PFPn) or perfluorohexane (PFH) followed by bath sonication. PSANDs had average size of around 200 nm. PFH/ PFPn leakage was then tested *in vitro* at 37 °C. PFH/ PFPn were retained in PSANDs at least for 1 hr. The PSANDs could be turned from liquid to gas by TUS irradiation. The extent of the phase shift depended more on the US frequency than the intensity. Maximum contrast enhancement was achieved with TUS intensity about 2 W/cm^2 for (PFPn) PSANDs, and 5 W/cm^2 for (PFH)PSANDs.

These results suggest that UCAs with proper size and high drug loading can be prepared with fairly simple means. Therefore, these UCAs can be easily and effectively be used in the field of drug delivery and cancer theranostic.

II. Application of phospholipid-based ultrasound contrast agents for gene delivery and cancer theranostics

Based on the findings presented in Chapter I, two main applications were decided. The first application was employment of MFBs for gene transfection. MFBs were mixed with plasmid DNA and intravenously injected into mice followed by TUS irradiation on the left limb muscles. The gene expression was significantly higher than that in the mice treated with plasmid DNA and TUS only. Moreover, aged MFBs that left for 24 hr at RT or at 4 ℃ for several days were found to still be functional in enhancing the gene expression in mice limb muscles. The second application was the utilisation of the DLBs as a theranostic agent in tumour bearing mice. The inhibitory

effect on the proliferation of murine B16BL6 melanoma cells *in vitro* was enhanced using a combination of TUS irradiation and DLBs compared to that with only DLBs treatment. Moreover, *in vivo*, DLBs in combination with TUS significantly inhibited the growth of B16BL6 melanoma tumour in mice. Additionally, ultrasonography showed high contrast enhancement of the DLBs in the tumour vasculature. Also, I evaluated the stability of (PFH)PSANDs in mice after systematic admistiration in tumour bearing mice. Gas chromatography analysis showed that PFH can be sustained in circulation as well as in tumour for 15 min after intravenous injection. Moreover, the ultrasonography imaging in mouse carotid artery indicated that droplets could shift to bubbles after TUS irradiation leading to a contrast signal enhancement at the imaging site. Finally, the direct intratumoral inection of (PFPn)PSANDs followed by low-intensity TUS led to temperature increase in the tumour site. And subsequently, the tumour volume was significantly reduced possibly due to both mechanical and thermal effects generated form PSANDs cavitation. These results indicated the possibility of using PSANDs in both systemic and loacal (intratumoral) routes; thus more effective theranostic outcomes can be achieved.

In conclusion, this research is one of the first attempts in highlighting the theranostic potential of UCAs toward more advanced biomedical applications. Accordingly, I have developed several methods for producing different theranostic UCAs starting with phospholipids and (gas/liquid) PFCs. These UCAs have been tested *in vitro* and *in vivo* and have been shown to be effective as therapeutic and diagnostic agents in applications like gene delivery and cancer treatment.

Acknowledgment

The author would like to express his sincere gratitude to Professor Mitsuru Hashida for his support throughout the many years of the PhD course, keeping me going when times were tough, asking insightful questions, and offering invaluable advice.

The author also expresses his thanks to Associate Professor Fumiyoshi Yamashita and Lecturer Yuriko Higuchi for their useful discussions.

The author would like to deeply thanks Professor Kazuo Maruyama (Teikyo University, Faculty of Pharma Sciences, Tokyo), Associate Professor Ryo Suzuki (Teikyo University, Faculty of Pharma Sciences, Tokyo), Research Associate Johan Unga (Teikyo University, Faculty of Pharma Sciences, Tokyo), and Research Associate Yusuke Oda (Teikyo University, Faculty of Pharma Sciences, Tokyo) for their kind support and advice concerning ultrsonography imaging and other related research.

The author expresses his great thanks to Professor Shigeru Kawakami (Nagasaki University, Graduate School of Biomedical Sciences, Nagasaki) for the useful advice and the valuable discussions.

The author would like to thank his laboratory mates and the secretaries in the Department of Drug Delivery Research for their kind support.

The author would like to express his thanks to his friends and family for their warm support in hard times.

Finally, the author wants to express his love and gratitude to his beloved parents and siblings; because without their support none of this would have been possible.

References

[1] O. Tacar, P. Sriamornsak, C.R. Dass, Doxorubicin: An update on anticancer molecular action, toxicity and novel drug delivery systems, J. Pharm. Pharmacol. 65 (2013) 157–170.

[2] Y. Ueno, S. Sonoda, R. Suzuki, M. Yokouchi, Y. Kawasoe, K. Tachibana, K. Maruyama, T. Sakamoto, S. Komiya, Combination of ultrasound and bubble liposome enhance the effect of doxorubicin and inhibit murine osteosarcoma growth., Cancer Biol. Ther. 12 (2011) 270–277.

[3] I. Lentacker, B. Geers, J. Demeester, S.C. De Smedt, N.N. Sanders, Design and evaluation of doxorubicin-containing microbubbles for ultrasound-triggered doxorubicin delivery: cytotoxicity and mechanisms involved., Mol. Ther. 18 (2010) 101–108.

[4] C.-H. Fan, C.-Y. Ting, H.-J. Lin, C.-H. Wang, H.-L. Liu, T.-C. Yen, C.-K. Yeh, SPIO-conjugated, doxorubicin-loaded microbubbles for concurrent MRI and focused-ultrasound enhanced brain-tumor drug delivery., Biomaterials. 34 (2013) 3706–15.

[5] S. Tinkov, G. Winter, C. Coester, R. Bekeredjian, New doxorubicin-loaded phospholipid microbubbles for targeted tumor therapy: Part I--Formulation development and in-vitro characterization., J. Control. Release. 143 (2010) 143–50.

[6] N. Sax, T. Kodama, Optimization of acoustic liposomes for improved in vitro and in vivo stability., Pharm. Res. 30 (2013) 218–24.

[7] S. Ibsen, M. Benchimol, S. Esener, Fluorescent microscope system to monitor real-time interactions between focused ultrasound, echogenic drug delivery vehicles, and live cell membranes, Ultrasonics. 53 (2013) 178–184.

[8] S. Tinkov, C. Coester, S. Serba, N.A. Geis, H.A. Katus, G. Winter, R. Bekeredjian, New doxorubicin-loaded phospholipid microbubbles for targeted tumor therapy: in-vivo characterization., J. Control. Release. 148 (2010) 368–72.

[9] C.D. Walkey, W.C.W. Chan, Cancer Theranostics, 2014.

[10] S. Svenson, Theranostics: Are we there yet?, Mol. Pharm. 10 (2013) 848–856.

[11] I. Lentacker, I. De Cock, R. Deckers, S.C. De Smedt, C.T.W. Moonen, Understanding ultrasound induced sonoporation: Definitions and underlying mechanisms, Adv. Drug Deliv. Rev. 72 (2014) 49–64.

[12] R. Lencioni, F. Piscaglia, L. Bolondi, Contrast-enhanced ultrasound in the diagnosis of hepatocellular carcinoma, J. Hepatol. 48 (2008) 848–857.

[13] M.A. Pysz, I. Guracar, K. Foygel, L. Tian, J.K. Willmann, Quantitative assessment of

tumor angiogenesis using real-time motion-compensated contrast-enhanced ultrasound imaging, Angiogenesis. 15 (2012) 433–442.

[14] S.R. Sirsi, M.L. Flexman, F. Vlachos, J. Huang, S.L. Hernandez, H.K. Kim, T.B. Johung, J.W. Gander, A.R. Reichstein, B.S. Lampl, A. Wang, A.H. Hielscher, J.J. Kandel, D.J. Yamashiro, M.A. Borden, Contrast Ultrasound Imaging for Identification of Early Responder Tumor Models to Anti-Angiogenic Therapy, Ultrasound Med. Biol. 38 (2012) 1019–1029.

[15] K. Ogawara, K. Un, K. Tanaka, K. Higaki, T. Kimura, In vivo anti-tumor effect of PEG liposomal doxorubicin (DOX) in DOX-resistant tumor-bearing mice: Involvement of cytotoxic effect on vascular endothelial cells., J. Control. Release. 133 (2009) 4–10.

[16] Y. Negishi, N. Hamano, Y. Tsunoda, Y. Oda, B. Choijamts, Y. Endo-Takahashi, D. Omata, R. Suzuki, K. Maruyama, M. Nomizu, M. Emoto, Y. Aramaki, AG73-modified Bubble liposomes for targeted ultrasound imaging of tumor neovasculature, Biomaterials. 34 (2013) 501–507.

[17] X. Dai, Z. Yue, M.E. Eccleston, J. Swartling, N.K.H. Slater, C.F. Kaminski, Fluorescence intensity and lifetime imaging of free and micellar-encapsulated doxorubicin in living cells., Nanomedicine. 4 (2008) 49–56.

[18] M.J. McKeage, B.C. Baguley, Disrupting established tumor blood vessels: An emerging therapeutic strategy for cancer, Cancer. 116 (2010) 1859–1871.

[19] R.J. Price, D.M. Skyba, S. Kaul, T.C. Skalak, Delivery of colloidal particles and red blood cells to tissue through microvessel ruptures created by targeted microbubble destruction with ultrasound., Circulation. 98 (1998) 1264–1267.